Negative potential-induced scalarization in the Einstein-Euler-Heisenberg black hole*

Hong Guo (郭弘)[1†] Miok Park[1‡] Yun Soo Myung[2§]

[1]Particle Theory and Cosmology Group, Center for Theoretical Physics of the Universe, Institute for Basic Science (IBS), Daejeon 34126, Korea
[2]Center for Quantum Spacetime, Sogang University, Seoul 04107, Korea

Abstract: We investigate a negative potential-induced scalarization of the Einstein-Euler-Heisenberg (EEH) black hole in the EEH-scalar theory, characterized by mass M, Euler-Heisenberg parameter μ, and magnetic charge q. In the regime $\mu > \mu_{\rm max} = 0.019$ (with $M = 1/2$), the black hole admits a single horizon and allows for overcharged configurations with $q/M > 1$. We obtain a single branch of scalarized EEH (sEEH) black holes for $q > 0$, which is considered as the simplest model for scalarization of EEH black holes. We find that this class of hairy black holes is not thermodynamically favored, and their quasinormal modes indicate that they are dynamically unstable. A notable feature is that the scalar charge depends weakly on q for $q < 1/2$ but grows more rapidly for $q > 1/2$, suggesting a transition from primary- to secondary-type scalar charge. This finding reveals characteristic properties of hairy black holes in EEH theory, specifically in the overcharging regime.

Keywords: hairy black hole, scalarization, Einstein-Euler-Heisenberg theory

DOI: 10.1088/1674-1137/ae457c **CSTR:** 32044.14.ChinesePhysicsC.50065102

I. INTRODUCTION

A fundamental question in black hole physics is whether these objects can possess rich structures, often referred to as "hair." Following the development of the Uniqueness Theorem [1, 2], the no-hair conjecture was proposed, stating that a stationary, axisymmetric black hole is fully described by its mass, electric charge, and angular momentum [3]. This conjecture was later proven more rigorously by Bekenstein for the specific case of scalar fields, demonstrating that black holes cannot sustain scalar "hair" under certain conditions [4, 5]. However, evasions of the no-hair theorem have been found in theories of gravity that extend beyond general relativity (GR) or incorporate nonlinear matter fields. For a comprehensive review of these cases, we refer the reader to Refs. [6, 7].

Under these circumstances, various black holes with scalar hair have been numerically constructed in Einstein-Gauss-Bonnet-scalar theories [8−11] and Einstein-Maxwell-scalar (EMS) theories [12]. These solutions have inspired further studies aiming to understand the formation mechanisms of scalar hair from initially bald black holes. One such mechanism, known as spontaneous scalarization [9], suggests that a tachyonic instability—induced by an effective negative mass squared of the scalar perturbation—triggers the growth of a dynamical scalar field from a constant scalar background. However, the stability of the resulting hairy black holes must be examined independently for each case. Another work [11, 13] instead employed a scalar coupling function with mass and quartic interaction terms, demonstrating the possibility of a phase transition from black holes to hairy black holes via spontaneous symmetry breaking in a symmetry-broken phase. This alternative mechanism has the advantage of ensuring the stability of the final state.

An intriguing feature of the EMS theory [12] is the existence of overcharged black holes with charge-to-mass ratios $q \leq M$, which is significantly distinct from the case of Reissner-Nordström (RN) black holes. A similar feature appears in gravitational theories coupled to nonlinear electrodynamics. Euler and Heisenberg (EH) proposed a novel framework in which one-loop corrections are incorporated into quantum electrodynamics (QED), introducing an EH parameter $a = 8\alpha_{fs}/45m^4 (\equiv 8\mu)$ to explain the vacuum polarization in QED and control the

Received 12 January 2026; Accepted 13 February 2026; Accepted manuscript online 14 February 2026

* Y.S.M. was supported by the National Research Foundation of Korea (NRF) grant funded by the Korea government(MSIT) (RS-2022-NR069013). M.P. and H.G. were supported by the Institute for Basic Science (Grant No. IBS-R018-Y1)

† E-mail: guohong@ibs.re.kr
‡ E-mail: miokpark76@ibs.re.kr
§ E-mail: ysmyung@inje.ac.kr

strength of the nonlinear electrodynamics contribution [14]. Yajima and Tamaki later derived the Einstein-Euler-Heisenberg (EEH) black hole solution by considering the one-loop effective Lagrangian together with Einstein gravity [15]. In this theory, the black hole charge can naturally extend into the regime $q \geq M$ without any restrictive assumptions. It should be emphasized that the physics of black holes in the overcharged regime remains largely unexplored. This is an important open question, as it highlights issues related to naked singularities and the weak cosmic censorship conjecture [16−20]. In the context of the EEH gravity framework, it is also closely connected to the potential detection of quantum gravity effects [21−23].

In the EEH framework, it is interesting to explore whether black holes can support scalar hair. Analytical solutions for charged EEH black holes with scalar hair were recently found by introducing a specific scalar potential, with a scalar field profile characterized by $\phi(r) \sim \ln(1+\nu/r)$ [24]. In the present work, in contrast to the spontaneous scalarization mechanism that is triggered by tachyonic instability through the nonminimal scalar coupling to a higher-curvature term, we are instead motivated by Ref. [25] to investigate the scalarization of magnetically charged EEH black holes by adopting a negative scalar potential. Such negative higher-order polynomial potentials represent one of the simplest choices capable of inducing black hole scalarization in the Einstein-minimally coupled scalar theory. Unlike the commonly considered mass terms or quartic self-interaction terms, the emergence of a nontrivial scalar configuration does not rely on curvature couplings or an effective negative mass squared. Instead, it is directly driven by the dominance of the negative potential in the strong-gravity regime. The former induces infinite branches of scalarized black holes, while the latter provides a single branch of scalarized black holes. We aim to obtain scalarized EEH black holes (sEEH) and then analyze the distinct properties exhibited by magnetic charge within different parameter regimes.

Our results reveal that a negative scalar potential can trigger the formation of sEEH black holes, providing yet another example of a no-hair theorem evasion [6]. By solving the equations of motion, we obtain such a single branch of sEEH black hole solutions. We found that when the magnetic charge $q < 1/2$, the scalar charge varies only slightly with q for fixed M, whereas for $q > 1/2$, it increases more rapidly as q increases. This distinct behavior suggests that the scalar charge exhibits the characteristics of a primary charge for $q < 1/2$ and of a secondary charge for $q > 1/2$. It would be interesting in the future to more precisely examine whether the scalar charge is truly primary or not. We also investigated thermodynamic properties and the stability of these hairy black holes by analyzing their scalar perturbations and quasinormal modes (QNMs). Our findings indicate that this class of hairy black holes is neither thermodynamically favored nor dynamically stable. Nevertheless, these solutions provide a valuable theoretical framework for exploring nontrivial scalar field configurations on black holes. The negative potential itself might offer a mechanism for stable hairy black holes to lose their scalar hair.

II. EEHS THEORY AND ITS BLACK HOLE STABILITY

We introduce the Einstein-Euler-Heisenberg-scalar (EEHS) theory with a term $\mathcal{F}^2$:

$$S_{\rm EEHS} = \frac{1}{16\pi}\int {\rm d}^4x\sqrt{-g}\left[R - 2\partial_\mu\phi\partial^\mu\phi - V(\phi) - \mathcal{F} + \mu\mathcal{F}^2\right], \tag{1}$$

where the Maxwell term $\mathcal{F} = F_{\mu\nu}F^{\mu\nu}$ and the EH parameter is μ. The bald black hole solutions including μ were discussed extensively in the EEH theory without a scalar counterpart [15, 22, 26, 27]. The form of the scalar potential $V(\phi) = -4\alpha^2\phi^6$ is adopted from Ref. [25]. In the limit $q \to 0$, the present theory naturally reduces to that of Ref. [25].

We derive the Einstein equation from the action (1):

$$G_{\mu\nu} \equiv 2(T^{\phi}_{\mu\nu} + T^{F}_{\mu\nu}), \tag{2}$$

where two energy-momentum tensors take the forms

$$T^{\phi}_{\mu\nu} = \partial_\mu\phi\partial_\nu\phi - \frac{1}{2}\left[(\partial\phi)^2 + \frac{V(\phi)}{2}\right]g_{\mu\nu}, \tag{3}$$

$$T^{F}_{\mu\nu} = F_{\mu\rho}F_{\nu}{}^{\rho} - \frac{1}{4}\mathcal{F}g_{\mu\nu} - 2\mu\mathcal{F}F_{\mu\rho}F^{\rho}_{\nu} + \frac{\mu}{4}\mathcal{F}^2 g_{\mu\nu}. \tag{4}$$

The Maxwell equation leads to

$$\nabla_\mu(F^{\mu\nu} - 2\mu\mathcal{F}F^{\mu\nu}) = 0. \tag{5}$$

Interestingly, the scalar equation takes a simple form, characteristic of a minimally coupled scalar theory

$$\Box\phi = \frac{V'(\phi)}{4}. \tag{6}$$

First, let us introduce the mass function $\bar{m}(r)$ together with the magnetic field strength $\bar{\mathcal{F}} = 2q^2/r^4$ and $\bar{\phi} = 0$. In this case, the $T_t{}^t$-component of the Einstein equation re-

duces to

$$\bar{m}'(r) = \frac{q^2}{2r^2} - \mu\frac{q^4}{r^6}. \tag{7}$$

Solving this leads to the EEH black hole solution

$$\mathrm{d}s^2_{\rm EEH} = \bar{g}_{\mu\nu}\mathrm{d}x^\mu \mathrm{d}x^\nu = -f(r)\mathrm{d}t^2 + \frac{\mathrm{d}r^2}{f(r)} + r^2\mathrm{d}\Omega_2^2 \tag{8}$$

with

$$f(r) \equiv 1 - \frac{2\bar{m}(r)}{r} = 1 - \frac{2M}{r} + \frac{q^2}{r^2} - \frac{2\mu q^4}{5r^6}. \tag{9}$$

This black hole solution could be described by a set of three parameters (M,q,μ), where M denotes the ADM mass, q is the magnetic charge, and μ is the EH parameter. It should be noted that, in the $\mu \to 0$ limit, the metric of the EEH theory reduces to that of the RN black hole. Because our model is formulated with a purely radial magnetic field, the simplified theory corresponds to a magnetically charged RN black hole, which is mathematically identical to the standard electrically charged RN solution under spherical symmetry. In the following analysis, we fix $M = 0.5$ to maintain consistency with the existing literature.

Assuming $q > 0$, $M > 0$, and $\mu > 0$, the solution yields three real positive roots under the following conditions:

a. $(0 < \gamma < 1)$ $0 < \mu < x_1 + x_2$, or

b. $(1 < \gamma < 1.02)$ $x_1 - x_2 < \mu < x_1 + x_2$,

where we introduce the charge-to-mass ratio by $q = \gamma M$, while x_1 and x_2 are given by

$$x_1 = \left(-\frac{5.35837}{\gamma^4} + 0.37037\gamma^2 + \frac{9.64506}{\gamma^2} - 4.62963\right)M^2, \tag{10}$$

$$\begin{aligned} x_2 = \frac{0.00171468M^2}{\gamma^4}\Big(&-1.11974\times10^6\gamma^{10} + 9.72 \\ &\times10^6\gamma^8 - 3.1725\times10^7\gamma^6 + 4.85156\times10^7\gamma^4 - 3.51563 \\ &\times10^7\gamma^2 + 9.76563\times10^6\Big)^{\frac{1}{2}}. \end{aligned} \tag{11}$$

If $M = 0.5$ is fixed, the square root in x_2 requires $0 < \gamma \lesssim 1.02$. Because $x_1 + x_2$ increases with increasing γ, the parameter μ reaches its maximum value, $\mu_{\rm max} \sim 0.019$, at $\gamma \sim 1.02$, corresponding to the point where two roots become degenerate. Therefore, three real positive roots exist only when the charge-to-mass ratio satisfies $0 < \gamma \lesssim 1.02$. If μ exceeds $\mu_{\rm max} \sim 0.019$, then only a single real positive root exists for all values of γ. This corresponds to the case where the charge-to-mass ratio is unbounded, in sharp contrast to the RN black hole ($\mu = 0$, i.e., without QED effects), which possesses outer and inner horizons given by $r_{\rm RN\pm}(M,q) = M \pm \sqrt{M^2 - q^2}$. As demonstrated in Fig. 1, we set $\mu = 0.001, 0.01, 0.19$, and 0.3 as examples to illustrate this relationship.

Hereafter, we fix the EH parameter $\mu = 0.3$ to obtain a black hole with a single horizon. In this setting, we do not worry about the no scalar-haired inner horizon theorem, which corresponds to a no-go theorem for the scalar-haired Cauchy horizon [28]. This is one of the motivations for studying black hole scalarization in the regime of unbounded magnetic charge.

Before proceeding, we derive the temperature from the surface gravity as

$$\frac{f'(r)}{4\pi}\Big|_{r\to r_+} \to \tilde{T}(M,q) = \frac{1}{4\pi}\left[\frac{0.6q^4}{r_+^7(M,q)} - \frac{q^2}{r_+^3(M,q)} + \frac{1}{r_+(M,q)}\right], \tag{12}$$

where the last two terms represent the temperature $\tilde{T}_{\rm RN}(M,q)$ for the RN black hole (see Fig. 2 (left)). Also, the area-law entropy for EEH black hole is defined by

$$\tilde{a}_H = \pi r_+^2(M,q) \tag{13}$$

with its minimum of 1.06 occurring at $q = 0.7$ with $M = 0.5$ (see Fig. 2 (right)).

We now introduce perturbations around the EEH black hole

$$g_{\mu\nu} = \bar{g}_{\mu\nu} + h_{\mu\nu}, \quad \phi = 0 + \delta\varphi, \quad F_{\mu\nu} = \bar{F}_{\mu\nu} + f_{\mu\nu} \tag{14}$$

with a metric perturbation $h_{\mu\nu}$ and linearized Maxwell field $f_{\mu\nu} = \partial_\mu a_\nu - \partial_\nu a_\mu$. The linearized scalar equation takes the form

$$\bar{\Box}\delta\varphi = 0. \tag{15}$$

Our task is to solve the linearized scalar equation (15) to examine the (in)stability of the EEH black hole. This is because its linearized metric theory has been shown to be stable against metric perturbations around EEH black holes [29]. The latter conclusion was reached through the computation of QNM frequencies for both axial and polar metric perturbations, which differ from those of RN black holes.

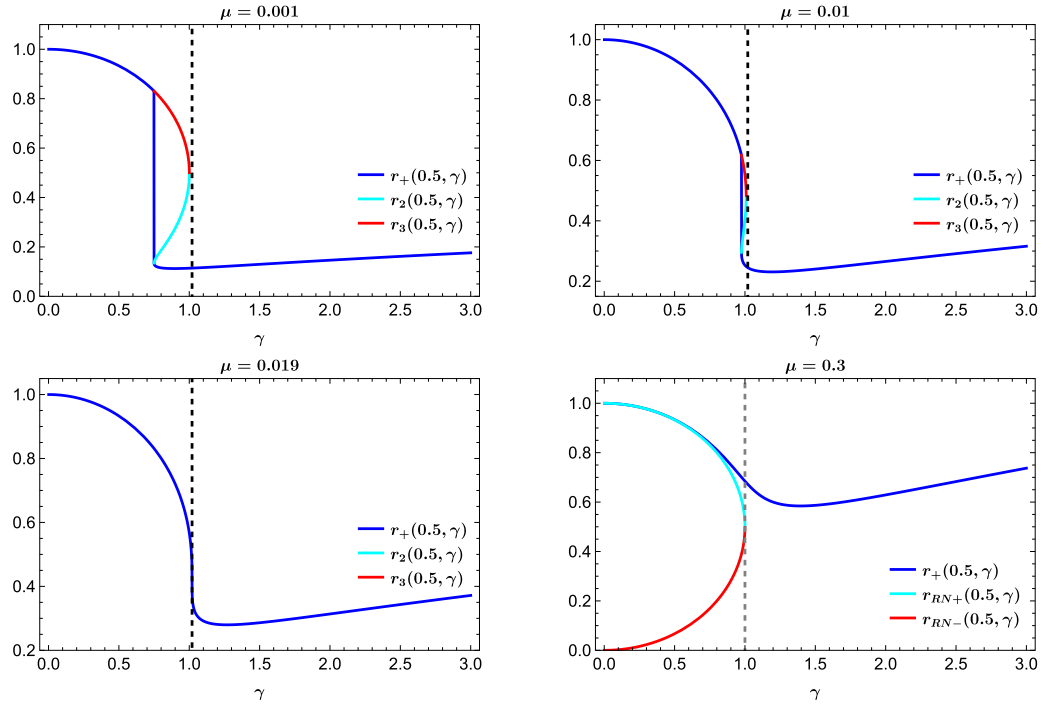

Fig. 1. (color online) Parameter γ represents the charge-to-mass ratio, with the dashed black line indicating $\gamma = 1.02$. In the EEH black hole, three distinct real positive horizons exist only when $\mu \lesssim 0.019$, as shown in the top and bottom-left figures. When a single horizon exists $\mu > 0.019$, its size is compared with that of an RN black hole of the same ADM mass ($M = 0.5$) in the bottom-right figure.

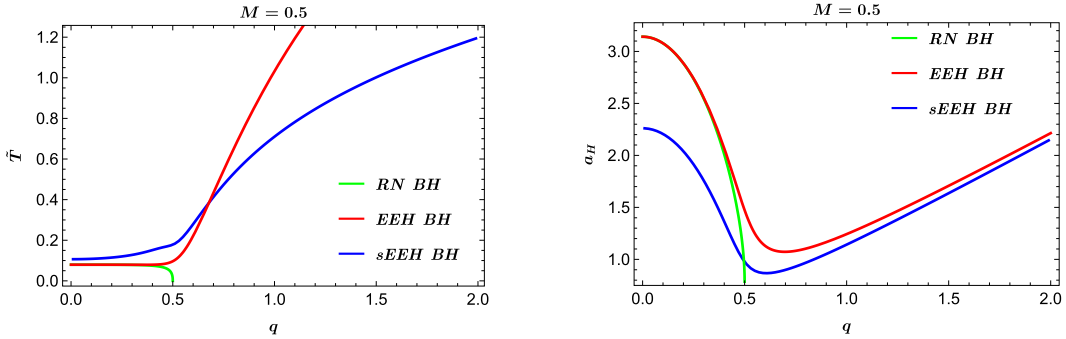

Fig. 2. (color online) (left) Temperatures $\tilde{T}(M = 0.5, q)$, $T(M = 0.5, q)$, and $\tilde{T}_{\rm RN}(M = 0.5, q)$ as functions of q for EEH, sEEH, and RN ($\mu = 0$) black holes. The first two are increasing functions, while the last is a decreasing function. The minimum temperature (=0.08) for an EEH black hole is located at $q = 0.35$, while the minimum temperature (=0) for an RN black hole is at an extremal point ($q = 0.5$). (right) Area-law entropy of the outer horizon as functions of q with $M = 0.5$ for EEH, sEEH, and RN ($\mu = 0$) black holes. The minimum entropy (=1.06) is located at $q = 0.7$ for EEH black holes.

Considering a separation of variables

$$\delta\varphi(t,r,\theta,\hat{\phi}) = \int \sum_{lm} \varphi(r) Y_{lm}(\theta) e^{im\hat{\phi}} e^{-i\omega t} d\Omega,$$
$$\varphi(r) = \frac{u(r)}{r}, \tag{16}$$

which transforms Eq. (15) into a Schrödinger-type equation in terms of the tortoise coordinate $r_* = \int \frac{dr}{f(r)}$,

$$\frac{d^2u(r)}{dr_*^2} + \left[\omega^2 - V_{\rm EEH}(r,M,q)\right] u(r) = 0. \tag{17}$$

Here, the effective scalar potential is given by

$$V_{\rm EEH}(r,M,q) = f(r)\left[\frac{l(l+1)}{r^2} + \frac{2M}{r^3} - \frac{2q^2}{r^4} + \frac{3.6q^4}{5r^8}\right]. \tag{18}$$

In the following, we focus on the $s(l = 0)$-mode scalar perturbation for further analysis (see Fig. 3 (left) for its q-

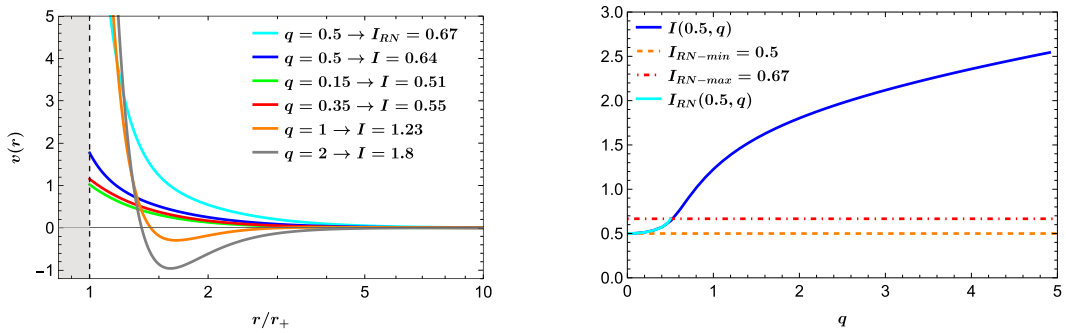

Fig. 3. (color online) Potential $v(r,M,q)$ and its integration $I(M,q)$. (left) Five q-dependent potentials $v(r,M=0.5,q)$ as functions of r/r_+ with $q=0.15,0.35,0.5,1,2$. Negative regions appear near the horizon for $q>0.5$. However, $v_{\rm RN}(r,0.5,q)$ is a positive function of $r\in[r_{\rm RN+},\infty]$ for $q\in[0,0.5]$. (right) Integration $I(0.5,q)$ as a function of q. Its lower limit is 0.5 at $q=0.0001$, and I grows monotonically with increasing q. We note that $I_{\rm RN}(0.5,0)=0.5$ is considered as the minimum and $I_{\rm RN}(0.5,0.5)=0.67$ is regarded as its maximum.

dependent potential profiles $v(r,M,q)$). A sufficient condition for instability is given by [30]

$$\int_{r_+(M,q)}^{\infty}\left[\frac{V_{\rm EEH}(r,M,q)}{f(r)}\right]{\rm d}r=\int_{r_+(M,q)}^{\infty}v(r,M,q){\rm d}r\equiv I(M,q)<0. \tag{19}$$

Although $v(r,0.5,q)$ develops negative regions near the horizon as q increases, these negative contributions are insufficient to trigger an instability. Indeed, Fig. 3 (right) shows clearly that $I(0.5,q)\geq 0.5$ for all $q>0$, confirming the stability of the EEH black hole. For the RN black hole with $\mu=0$, $v_{\rm RN}(r,0.5,q)$ remains strictly positive for $r\in[r_{\rm RN+},\infty]$ within $q\in[0,0.5]$. Its integral attains a minimum value of 0.5 at $q=0$ and maximum of 0.67 at $q=0.5$.

III. sEEH BLACK HOLES AND THEIR PROPERTIES

Let us derive sEEH black holes through negative potential-induced scalarization by solving the full set of equations. For this purpose, we adopt the following metric and field ansatz [12]:

$$\begin{aligned}&{\rm d}s^2_{\rm sEEH}=-N(r){\rm e}^{-2\delta(r)}{\rm d}t^2+\frac{{\rm d}r^2}{N(r)}+r^2(d\theta^2+\sin^2\theta d\hat{\varphi}^2)\\&N(r)=1-\frac{2m(r)}{r},\quad \phi=\phi(r),\quad A=A_{\hat{\varphi}}d\hat{\varphi}.\end{aligned} \tag{20}$$

Substituting the gauge field ansatz into Eq. (5) yields the magnetic potential $A_{\hat{\varphi}}=-q\cos\theta$, which in turn gives $F_{\theta\hat{\varphi}}=q\sin\theta$ and $\mathcal{F}=2q^2/r^4$. This implies that no approximation for $A_{\hat{\varphi}}$ is required; the nonlinear Maxwell equation is solved exactly in this case. Substituting Eq. (20) into Eqs. (2) and (6), one finds three equations for $m(r)$, $\delta(r)$, and $\phi(r)$:

$$m'(r)=\frac{q^2}{2r^2}-\frac{0.3q^4}{r^6}+\frac{r^2}{2}\left[\left(1-\frac{2m(r)}{r}\right)\phi'^2(r)-\frac{V(\phi)}{2}\right], \tag{21}$$

$$\delta'(r)=-r\phi'^2(r), \tag{22}$$

$$\begin{aligned}&\frac{2}{r^2}\left[m(r)+rm'(r)-r\right]\phi'(r)\\&+\left(1-\frac{2m(r)}{r}\right)[\delta'(r)\phi'(r)-\phi''(r)]=-\frac{V'(\phi)}{4},\end{aligned} \tag{23}$$

where the prime ($'$) denotes differentiation with respect to its argument. We note that Eq. (21) reduces to Eq. (7) when $\phi(r)=0$. Considering the existence of a single horizon located at $r=r_+$, the near-horizon behavior of the solution to Eqs. (21)–(23) can be expressed as

$$m(r)=\frac{r_+}{2}+m_1(r-r_+)+\cdots,\quad \delta(r)=\delta_1(r-r_+)+\cdots, \tag{24}$$

$$\phi(r)=\phi_0+\phi_1(r-r_+)+\cdots, \tag{25}$$

where the expansion coefficients are given by

$$\begin{aligned}&m_1=\frac{q^2}{2r_+^2}-\frac{0.3q^4}{r_+^6}+\frac{r_+^2V(\phi_+)}{4},\quad \delta_1=-r_+\phi_1^2,\\&\phi_1=\frac{r_+V'(\phi_+)}{4(1-2m_1)}.\end{aligned} \tag{26}$$

Here, the constant scalar $\phi_0\equiv\phi(r_+)$ will be determined when matching with an asymptotically flat solution in the far region

$$m(r) = M - \frac{q^2+q_s^2}{2r} + \cdots, \quad \delta(r) = \delta_0 + \frac{q_s^2}{2r^2} + \cdots,$$
$$\phi(r) = \frac{q_s}{r} + \cdots, \tag{27}$$

where M is the ADM mass, q is the magnetic charge, and q_s denotes the scalar charge.

Near the horizon, $\phi(r,q)$ is determined by three free parameters: r_+, q, and ϕ_0. Using the shooting method to enforce $\phi(r\to\infty,q)=0$ and $m(r\to\infty,q)=1/2$, we can fix both ϕ_0 and r_+. As a result, all numerical solutions are effectively characterized by tuning a single free parameter q. It is worth noting that, contrary to the situation of infinite branches found in the EMS theory, the EEHS theory considered here admits the single branch of scalarized black hole solutions. Regarding explicit sEEH black hole solutions with $q=0.15,0.35,0.5,1,2$, we present numerical results for the single branch with $M=0.5,\mu=0.3$, $\alpha=1$. As shown in Fig. 4, the scalar field $\phi(r,q)$ decreases monotonically with r, while $\delta(r,q)$ are negative monotonically decreasing functions of r. Meanwhile, by setting $\delta(r_+,q)=0$, $\delta(r,q)$ decreases monotonically in the near-horizon region. At large r, the asymptotic behavior of $\delta(r,q)$ depends on whether $q\leqslant 0.5$ or $q>0.5$, consistent with the behavior of $\phi(r,q)$. These functions vanish identically for EEH black holes.

For comparison, Fig. 5 display the two mass functions $\tilde{m}(r,q)$ for an EEH black hole and $m(r)$ for an sEEH black hole with $q=0.15,0.35,0.5,1,2$. In both cases, the mass functions asymptotically approach $M=0.5$ at large r, and a negative region emerges for $q\gtrsim 1$. Although sEEH black holes exhibit a deeper potential well compared to EEH black holes with the same q, the two solutions remain qualitatively similar.

In Fig. 2 (left), we present three temperature profiles for EEH, sEEH, and RN black holes as functions of q. The temperatures $\tilde{T}(M=0.5,q)$ and $\tilde{T}_{\rm RN}(M=0.5,q)$ correspond to the EEH and RN black holes, respectively, with the former increasing and latter decreasing as functions of q. The EEH black hole reaches its minimum temperature $\tilde{T}=0.08$ at $q=0.35$, whereas the RN black hole's minimum temperature $\tilde{T}_{\rm RN}$=0 at extremal point ($q=0.5$). The temperature for sEEH black holes is defined by

$$T(M,q) = \frac{1}{4\pi}N'(r_+)e^{-\delta(r_+)}, \tag{28}$$

which increases with q, resembling the behavior of $\tilde{T}(M,q)$ for the EEH black hole. Its minimum temperature occurs near $q\simeq 0$.

Fig. 2 (right) shows the area-law entropy of the outer horizon as a function of q with $M=0.5$. It is defined as

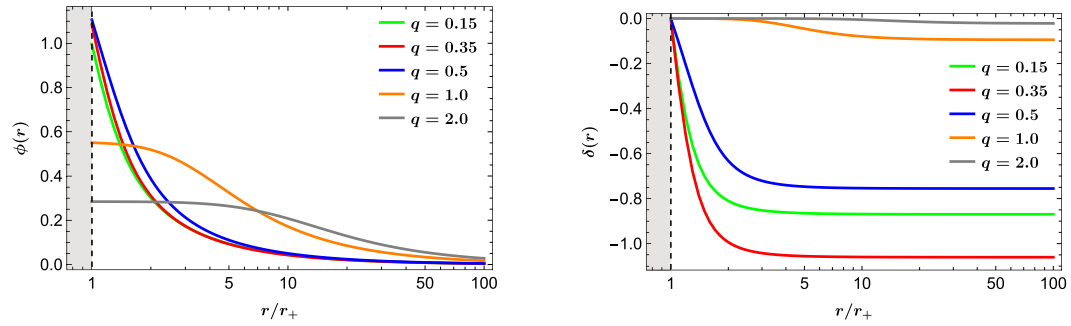

Fig. 4. (color online) (left) Scalar hair $\phi(r\in[r_+,100],q)$ with $q=0.15,0.35,0.5,1,2$. These are decreasing functions of r with different initial values at $r=r_+$. (right) $\delta(r\in[r_+,100],q)$ with different $q=0.15,0.35,0.5,1,2$, are negative decreasing functions of r.

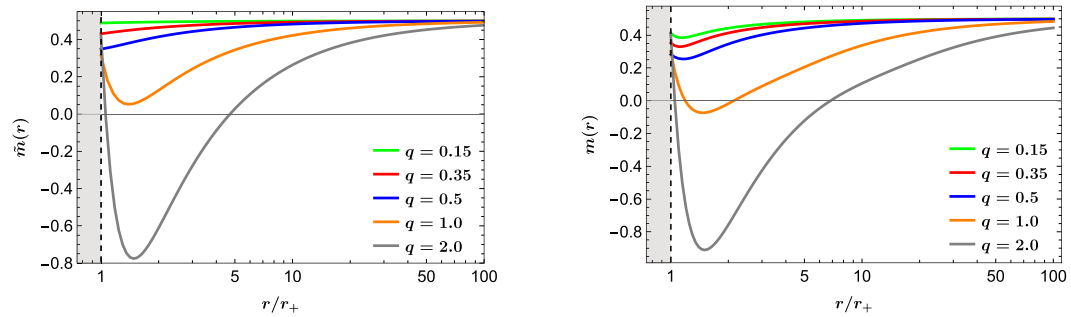

Fig. 5. (color online) (left) Mass function $\tilde{m}(r\in[r_+,100],M=0.5,q)$ with $q=0.15,0.35,0.5,1,2$ for EEH black hole. They all converge $M=0.5$ at large r. Negative regions appear for $q=2$. (right) Mass function $m(r\in[r_+,100],q)$ for sEEH black hole with $\alpha=1$. Negative regions appear for $q=1,2$.

$$a_H(M,q) = \pi r_+^2. \tag{29}$$

Here, we observe the inequality $a_H(M=0.5,q) < \tilde{a}_H(M=0.5,q)$ for $q>0$, implying that sEEH black holes represent less thermodynamically favorable configurations compared to EEH black holes. Within the restricted interval $0<q<0.5$, the entropy ordering is $a_H < \tilde{a}_H^{\rm RN} < \tilde{a}_H$, which suggests that the EEH black hole remains the most thermodynamically preferred state in this range. The minimum entropy for EEH black holes is 1.06 at $q=0.7(>0.5)$, whereas the sEEH black hole attains a lower minimum entropy of 0.87 located at $q=0.61(<0.7)$. For RN black holes, the minimum entropy 0.79 occurs at $q=0.5$, while its maximum 3.14 is at $q=0$.

In Fig. 6, we show the scalar charge $q_s(M=0.5,q)$ and scalar constant $\phi_0(M=0.5,q)$ as functions of q. We found that $q_s(M=0.5,q)$ varies only slightly with q for $q<0.5$, while it increases more rapidly when $q>0.5$. This behavior corresponds to the differing scalar slopes observed for various q in Fig. 4 (left). Notably, this suggests that the scalar field exhibits the characteristics of a primary charge for $q\le 0.5$, whereas the growth of $q_s(q)$ for $q>0.5$ indicates a secondary scalar charge. This result represents a novel feature of sEEH black holes.

Meanwhile, the scalar constant $\phi_0(M=0.5,q)$ increases with q for $q<0.5$, attains a maximum near $q=0.5$, and then decreases for $q>0.5$. This behavior reflects the distinct initial scalar hair configurations at the horizon $r/r_+=1$, as shown in Fig. 4 (left). It is worth noting that in the limit $q\to 0$, our theory reduces to the Einstein–Klein–Gordon theory [25]. The above analysis confirms that hairy black hole solutions exist in this limit, in agreement with the results reported in Ref. [25].

Finally, we consider the energy density $\rho(r)$ to preliminarily assess the stability of sEEH black holes:

$$\rho(r) = -T_t^{\phi\, t} - T_t^{F\, t} = \frac{N(r)\phi'^2(r)}{2} - \phi^6(r) + \frac{m'(r)}{r^2}. \tag{30}$$

In case of $\phi=0$, Eq. (30) reduces to $\tilde{\rho}(r) = \dfrac{\tilde{m}'(r)}{r^2} = \dfrac{q^2}{2r^4} - \dfrac{0.3q^4}{r^8}$ for the EEH black hole in Eq. (7). Its behaviors are depicted in Fig. 7 (left) with $q=0.15,0.35,0.5,1,2$, along with the energy density for RN black holes ($\mu=0$). We observes a negative region near the horizon for $q>0.5$, indicating a violation of the weak energy con-

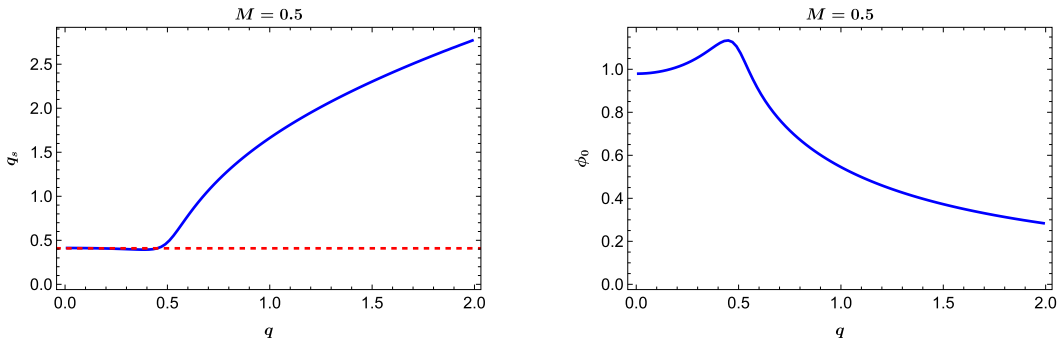

Fig. 6. (color online) (left) Constant scalar charge and scalar charge $q_s(M=0.5,q)$ as an increasing function of q for sEEH black holes. (right) Scalar constant $\phi_0(M=0.5,q)$ starting with an increasing function of q. This decreases for larger values of q in sEEH black holes.

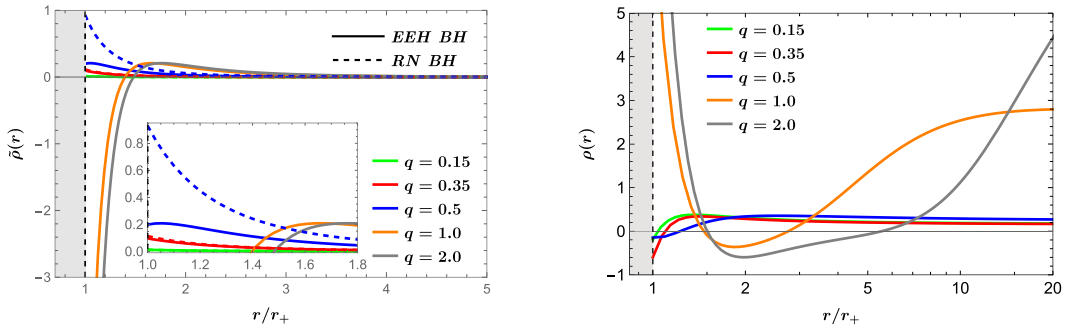

Fig. 7. (color online) Energy density $\rho(r,q)$ as a function of r/r_+. (left) Five profiles $\tilde{\rho}(r,q)$ as functions of $r/r_+\in[1,5]$ with $q=0.15,0.35,0.5,1,2$ for EEH black holes, together with the energy density of RN black hole ($\mu=0$) $\tilde{\rho}_{\rm RN}(r,q)=q^2/2r^4$ over $r/r_+\in[1,5]$. Negative regions appear near the horizon for $q>0.5$. In contrast, $\tilde{\rho}_{\rm RN}(r,0.5)$ remains positive for all r and is nearly the same as $\tilde{\rho}(r,0.5)$ for $r/r_+>2$. (right) Five profiles $\rho(r,M=0.5,q)$ as functions of $r/r_+\in[1,20]$ with $q=0.15,0.35,0.5,1,2$ for sEEH black holes. All cases exhibit negative energy density regions.

dition (WEC) for EEH black holes. However, this violation alone does not imply instability, since violation of the WEC is only one possible signal of instability. This is analogous to the negativity of $v(r,0.5,q)$ near the horizon for $q>0.5$ in EEH black holes (see Fig. 3 (left)). On the other hand, for sEEH black holes, negative energy density regions appear near the horizon when $q\leq 0.5$, while for $q>0.5$ such negative regions shift to an intermediate radial range. In all cases, the energy density for sEEH black holes includes negative regions, thus violating the WEC. These differences from the EEH black holes arise from the presence of the negative scalar potential.

IV. DYNAMICAL STABILITY FOR THE SINGLE BRANCH

We need to explore a wide range of numerical solutions as functions of q for the single branch to perform stability analysis of sEEH black holes. Such an analysis is crucial, as it may determine their viability in describing realistic astrophysical configurations with scalar hair. Our conclusions regarding the stability of sEEH black holes against radial perturbations will be drawn from the examination of the qualitative behavior of the s-mode scalar potential as well as the calculation of the QNM frequencies for s-mode scalar perturbation.

There are several indications suggesting possible instability in sEEH black holes. First, the entropy inequality $a_H(0.5,q)<\tilde{a}_H(0.5,q)$ draws our attention, implying that EEH black holes are thermodynamically more favorable than their scalarized counterparts. Second, the energy density for sEEH black holes exhibits negative regions for $q>0$, signaling a violation of the WEC.

Here, we prefer to introduce the radial perturbations around the sEEH black holes as

$$\begin{aligned} \mathrm{d}s^2_{\rm rp} =& -N(r)\mathrm{e}^{-2\delta(r)}(1+\epsilon H_0)\mathrm{d}t^2 \\ &+\frac{\mathrm{d}r^2}{N(r)(1+\epsilon H_1)}+r^2(\mathrm{d}\theta^2+\sin^2\theta\mathrm{d}\hat{\varphi}^2), \\ \phi(t,r) =& \phi(r)+\epsilon\delta\tilde{\phi}(t,r), \end{aligned} \tag{31}$$

where $N(r)$, $\delta(r)$, and $\phi(r)$ denote the sEEH black hole background, while $H_0(t,r)$, $H_1(t,r)$, and $\delta\tilde{\phi}(t,r)$ represent the perturbations propagating on the numerical background. No perturbations are introduced for the gauge field $A_{\hat{\varphi}}$. From now on, we focus on the $l=0$(s-mode) scalar propagation, neglecting higher angular momentum modes ($l\neq 0$). In this case, the two perturbed metric fields $H_0(t,r), H_1(t,r)$ become redundant via a decoupling procedure, leaving a single linearized scalar equation.

Considering the separation of variables

$$\delta\tilde{\phi}(t,r)=\frac{\tilde{\varphi}(r)\mathrm{e}^{-\mathrm{i}\omega t}}{r}, \tag{32}$$

the s-model scalar perturbation reduces to a Schrödinger-type equation

$$\frac{\mathrm{d}^2\tilde{\varphi}(r)}{\mathrm{d}r_*^2}+\left[\omega^2-V_{\rm sEEH}(r,q)\right]\tilde{\varphi}(r)=0, \tag{33}$$

where r_* is the tortoise coordinate defined by

$$\frac{\mathrm{d}r_*}{\mathrm{d}r}=\frac{\mathrm{e}^{\delta(r)}}{N(r)}. \tag{34}$$

Here, its scalar potential is given by

$$\begin{aligned} V_{\rm sEEH}(r,q)=&\frac{N\mathrm{e}^{-2\delta}}{r}\Big[N'-N\delta'-2r^2\phi'^2(N'+N/r-N\delta') \\ &-24r^2\phi'\phi^5-30r\phi^4\Big]. \end{aligned} \tag{35}$$

As a consistency check, we verify that setting $\delta(r)=0$, $\phi(r)=0$, and $N(r)\to f(r)$ reduces $V_{\rm sEEH}(r,q)$ to the EEH potential $V_{\rm EEH}(r,M,q)$ in Eq. (18).

At this stage, we examine the behavior of the effective potential $V_{\rm sEEH}(r,q)$. Fig. 8 displays scalar potential $V_{\rm sEEH}(r,q)$ for $l=0$(s-mode) scalar with $q>0$ in the single branch. In the left panel, one observes that $V_{\rm sEEH}(r,q)$ develops negative regions near the event horizon for $q\leq 0.51$. In contrast, the right panel shows that for $q>0.5$, a potential barrier forms, followed by the emergence of a potential well in the intermediate radial region. However, the mere presence of a potential well does not, by itself, imply that the single branch with $q>0$ is unstable under radial perturbations.

To reach a definitive result, we need to compute the QNM frequency defined by $\omega=\omega_R+\mathrm{i}\omega_I$ subject to the standard boundary conditions: purely ingoing waves at the outer horizon and purely outgoing waves at spatial infinity. We determine ω using the pseudo-spectral method [31]. As the real part ω_R vanishes for all cases considered, only the imaginary part ω_I is plotted in Fig. 9. From the numerical results, different from the case of EEH and RN black holes, for the single branch of sEEH black holes with $q>0$, all imaginary parts satisfy $\omega_I(q)>0$, which signals instability. Thus, the instability is present for any nonzero magnetic charge $q>0$. Moreover, $\omega_I(q)$ increases monotonically with q up to a maximum near $q\approx 0.45$, exhibits a transition around $q\approx 0.5$, and then decreases monotonically for larger q. This trend closely follows the variation of the potential well depth in Fig. 8 and is also qualitatively similar to the behavior of the scalar constant $\phi_0(M=0.5,q)$ at the outer horizon, as shown in Fig. 6 (right). Meanwhile, we can see from Fig. 9 that RN ($0<q\leq 1/2$) and EEH ($0<q\leq 2$)

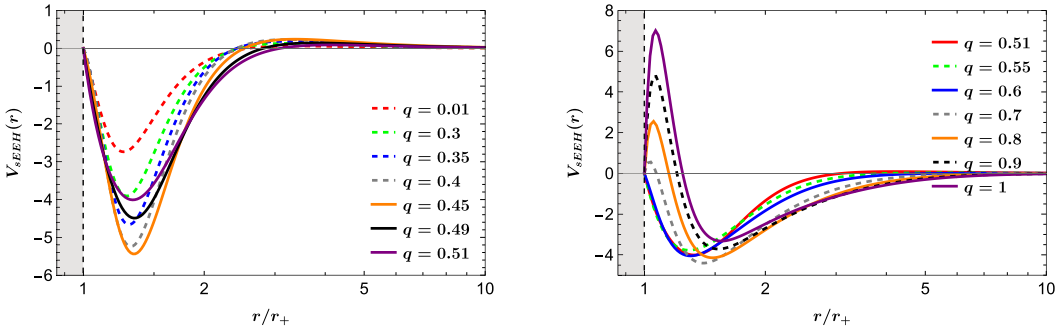

Fig. 8. (color online) (left) Scalar potentials $V_{\rm sEEH}(r,q)$ for $l=0$ scalar mode with various values of $q \le 0.51$ in the single branch. The potential well deepens as q increases and becomes shallower for $q > 0.45$. (right) As q increases from $q = 0.51$, a potential barrier first emerges, followed by the formation of a potential well in the intermediate region.

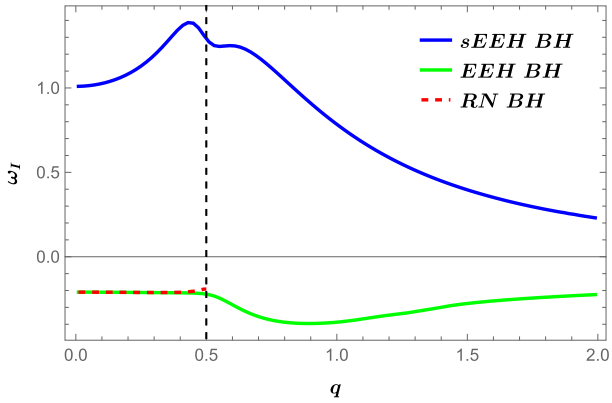

Fig. 9. (color online) Fundamental QNM frequency ω_I of the $l=0$ scalar mode as a function of q for sEEH black hole (blue), EEH black hole with $\alpha=0$ (green), and RN black hole with $\alpha=\mu=0$ (red). The black vertical dashed line represents $q=1/2$.

black holes are stable against radial perturbations because of their $\omega_I(q) < 0$, as predicted by Fig. 3 (right).

V. CONCLUSION AND FURTHER DISCUSSION

We have introduced the EEHS theory to investigate the scalarization of the EEH black hole described by mass M, EH parameter μ, and magnetic charge q. The EEH theory incorporates the one-loop effective Lagrangian of QED coupled to Einstein gravity [15]. It is worth noting that for $\mu > 0.019$ at $M = 0.5$, there is no restriction on the magnetic charge q for the existence of a single horizon. In the limiting case $\mu = 0$, the solution reduces to the RN black hole, which possesses both outer and inner horizons. For the present study, we set $\mu = 0.3$ so that the spacetime admits a single horizon.

To realize the simplest scalarization of the EEH black hole, we introduced a negative single term of the scalar potential $V(\phi) = -4\alpha^2\phi^6$ [25]. The onset scalarization does not occur for this black hole because it remians stable under scalar perturbations. However, the introduction of a negative potential can trigger scalarization, thereby providing a novel mechanism for evading the no-hair theorem [6]. By numerically solving the full set of three field equations, we obtained a single-branch family ($q > 0$) of sEEH black holes. Notably, there is no existence line separating scalarized and non-scalarized configurations in this case. A significant characteristic of sEEH black holes is that the scalar hair exhibits primary charge behavior for $q < 1/2$ and secondary charge behavior for $q > 1/2$ at a fixed ADM mass ($M = 0.5$). This distinctive property highlights a novel feature of these black holes.

Several indications point toward the instability of the sEEH branch. First, we note the entropy inequality $a_H(0.5,q) < \tilde{a}_H(0.5,q)$, which suggests that the EEH black hole is thermodynamically preferred over its scalarized counterpart. Second, the energy density of sEEH black holes exhibits negative regions for $q > 0$, signaling a violation of the WEC. We have further examined the stability of sEEH black holes by analyzing the s-mode scalar potential and computing the QNM frequencies under radial perturbations. In all cases with $q > 0$, the imaginary part of the QNM frequency satisfies $\omega_I(q) > 0$, indicating that the single branch of sEEH black holes is dynamically unstable against linearized scalar perturbations. Although introducing a negative scalar potential may violate the WEC [32, 33], and the potential instability under scalar perturbations could be closely tied to the negativity of the potential, such a setup nonetheless provides a valuable theoretical platform for exploring hairy black holes [32]. Regarding the final state implied by the dynamical instability of sEEH black holes, a plausible physical picture is that the system undergoes a descalarization process and eventually settles down to a hairless EEH black hole. Our results thus offer meaningful guidance for future investigations of dynamical scalarization and descalarization processes within this framework [34, 35], as well as for analyzing the associated dynamical instabilities.

It is worth noting that our results, as the simplest attempt at scalarization in the EEH gravity theory, highlight its substantial potential in the study of black hole

physics. The scalar charge exhibits a slight variation from a constant value with increasing q but undergoes a rapid increase as the black hole enters the overcharging regime, displaying a distinct property from primary to secondary hair characteristics. This behavior highlights the intricate and nontrivial structure inherent to the EEH theory. It further suggests that black holes in the overcharging regime, where the charge-to-mass ratio exceeds the extremal bound, may exhibit phenomena intimately connected to the principles of quantum gravity [36, 37] and the cosmic censorship conjecture [16−20]. Such connections are particularly significant for advancing our understanding of possible extensions or evasions of the classical black hole no-hair theorem. In this sense, the EEH theory offers a fertile testing ground for exploring the interplay between strong-field gravity, nonlinear electrodynamics, and quantum effects in extreme spacetimes.

ACKNOWLEDGMENTS

We appreciate APCTP for its hospitality during completion of this work.

References

[1] W. Israel, Phys. Rev. **164**(5), 1776 (1967)
[2] W. Israel, Commun. Math. Phys. **8**(3), 245 (1968)
[3] R. Ruffini and J. A. Wheeler, Phys. Today **24**(1), 30 (1971)
[4] J. D. Bekenstein, Phys. Rev. Lett. **28**, 452 (1972)
[5] J. D. Bekenstein, Phys. Rev. D **51**(12), R6608 (1995)
[6] C. A. R. Herdeiro and E. Radu, Int. J. Mod. Phys. D **24**(09), 1542014 (2015)
[7] M. S. Volkov, arXiv: 1601.08230
[8] D. D. Doneva and S. S. Yazadjiev, Phys. Rev. Lett. **120**(13), 131103 (2018)
[9] H. O. Silva, J. Sakstein, L. Gualtieri *et al*., Phys. Rev. Lett. **120**(13), 131104 (2018)
[10] G. Antoniou, A. Bakopoulos, and P. Kanti, Phys. Rev. Lett. **120**(13), 131102 (2018)
[11] B. Latosh and M. Park, Phys. Rev. D **110**(2), 024012 (2024)
[12] C. A. R. Herdeiro, E. Radu, N. Sanchis-Gual *et al*., Phys. Rev. Lett. **121**(10), 101102 (2018)
[13] Y. H. Hyun, B. Latosh, and M. Park, JHEP **08**, 163 (2024)
[14] W. Heisenberg and H. Euler, Z. Phys. **98**(11-12), 714 (1936)
[15] H. Yajima and T. Tamaki, Phys. Rev. D **63**, 064007 (2001)
[16] V. E. Hubeny, Phys. Rev. D **59**, 064013 (1999)
[17] C. Liu and S. Gao, Phys. Rev. D **101**(12), 124067 (2020)
[18] M. R. Alipour, S. Noori Gashti, B. Pourhassan *et al*., arXiv: 2504.03453
[19] A. Kehagias, K. D. Kokkotas, A. Riotto *et al*., Class. Quant. Grav. **41**(7), 075007 (2024)
[20] S. Shaymatov and B. Ahmedov, Gen. Rel. Grav. **55**(2), 36 (2023)
[21] G. Brodin, M. Marklund, and L. Stenflo, Phys. Rev. Lett. **87**, 171801 (2001)
[22] A. Allahyari, M. Khodadi, S. Vagnozzi *et al*., JCAP **02**, 003 (2020)
[23] S. I. Kruglov, Mod. Phys. Lett. A **35**(35), 2050291 (2020)
[24] T. Karakasis, G. Koutsoumbas, A. Machattou *et al*., Phys. Rev. D **106**(10), 104006 (2022)
[25] X. Y. Chew and Y. S. Myung, Phys. Rev. D **110**(4), 044011 (2024)
[26] D. Amaro and A. Macías, Phys. Rev. D **102**(10), 104054 (2020)
[27] N. Bretón and L. A. López, Phys. Rev. D **104**(2), 024064 (2021)
[28] D. O. Devecioglu and M. I. Park, Phys. Lett. B **829**, 137107 (2022)
[29] Z. Luo and J. Li, Chin. Phys. C **46**(8), 085107 (2022)
[30] G. Dotti and R. J. Gleiser, Class. Quant. Grav. **22**, L1 (2005)
[31] A. Jansen, Eur. Phys. J. Plus **132**(12), 546 (2017)
[32] T. Hertog, Phys. Rev. D **74**, 084008 (2006)
[33] K. A. Bronnikov, Particles **1**(1), 56 (2018)
[34] C. Y. Zhang, Q. Chen, Y. Liu *et al*., Phys. Rev. Lett. **128**(16), 161105 (2022)
[35] C. Y. Zhang, Q. Chen, Y. Liu *et al*., Phys. Rev. D **106**(6), L061501 (2022)
[36] F. Javed, Phys. Dark Univ. **44**, 101450 (2024)
[37] D. P. Sorokin, Fortsch. Phys. **70**(7-8), 2200092 (2022)